Achlorhydria by ezrin knockdown: defects in the formation/expansion of apical canaliculi in gastric parietal cells

Atsushi Tamura,[1] Shojiro Kikuchi,[1,2] Masaki Hata,[3] Tatsuya Katsuno,[1] Takeshi Matsui,[3] Hisayoshi Hayashi,[4] Yuichi Suzuki,[4] Tetsuo Noda,[5,6] Shoichiro Tsukita,[1] and Sachiko Tsukita[1,7]

[1]Department of Cell Biology, Faculty of Medicine, Kyoto University, Sakyo-ku, Kyoto 606-8501, Japan
[2]Department of Surgery, Kyoto Prefectural University of Medicine, Kamigyo-ku, Kyoto 602-8566, Japan
[3]KAN Research Institute, Kyoto Research Park, Shimogyo-ku, Kyoto 606-8317, Japan
[4]Laboratory of Physiology, School of Food and Nutritional Sciences, University of Shizuoka, Shizuoka 422-8526, Japan
[5]Department of Cell Biology, Cancer Institute of Japanese Foundation for Cancer Research, Koto-ku, Tokyo 135-8550, Japan
[6]Department of Molecular Genetics, Tohoku University School of Medicine, Seryo-cho, Aoba-ku, Sendai 980-8575, Japan
[7]School of Health Sciences, Faculty of Medicine, Kyoto University, Sakyo-ku, Kyoto 606-8507, Japan

Loss of gastric acid secretion is pathologically known as achlorhydria. Acid-secreting parietal cells are characterized by abundant expression of ezrin (*Vil2*), one of ezrin/radixin/moesin proteins, which generally cross-link actin filaments with plasma membrane proteins. Here, we show the direct in vivo involvement of ezrin in gastric acid secretion. Ezrin knockout ($Vil2^{-/-}$) mice did not survive >1.5 wk after birth, making difficult to examine gastric acid secretion. We then generated ezrin knockdown ($Vil2^{kd/kd}$) mice by introducing a neomycin resistance cassette between exons 2 and 3. $Vil2^{kd/kd}$ mice born at the expected Mendelian ratio exhibited growth retardation and a high mortality. Approximately 7% of $Vil2^{kd/kd}$ mice survived to adulthood. Ezrin protein levels in $Vil2^{kd/kd}$ stomachs decreased to <5% of the wild-type levels without compensatory up-regulation of radixin or moesin. Adult $Vil2^{kd/kd}$ mice suffered from severe achlorhydria. Immunofluorescence and electron microscopy revealed that this achlorhydria was caused by defects in the formation/expansion of canalicular apical membranes in gastric parietal cells.

Introduction

Gastric acid, i.e., hydrochloric acid (HCl), is secreted from highly differentiated gastric epithelial cells called "parietal" cells, which are characterized by numerous H^+,K^+-ATPase-rich tubulovesicles and mitochondria in the cytoplasm (Urushidani and Forte, 1997; Yao and Forte, 2003). This secretion is tightly regulated. In parietal cells, ligands such as acetylcholine, gastrin, and histamine bind to their receptors localizing at basolateral plasma membranes (Urushidani and Forte, 1997; Lindstrom et al., 2001; Yao and Forte, 2003). Protein kinase cascades are then activated, and H^+,K^+-ATPase-rich tubulovesicles are fused with apical membranes to generate and secrete HCl to the gastric lumen (Forte and Yao, 1996; Forte et al., 1977; Duman et al., 2002; Zhou et al., 2003). However, the molecular mechanisms underlying the regulation of this tubulovesicle fusion remain elusive. One of the characteristic features of parietal cells is the abundant expression of ezrin, which is concentrated at the subapical actin cortical layers (Hanzel et al., 1991; Urushidani and Forte, 1997; Yao and Forte, 2003). Thus, it has been speculated that ezrin functions as one of the key regulators for gastric acid secretion in parietal cells. Recently, the NH_2-terminal phosphorylation of ezrin was suggested to play a critical role in gastric acid secretion (Zhou et al., 2003). Ezrin belongs to the ezrin/radixin/moesin (ERM) family (Bretscher, 1983; Sato et al., 1992). ERM proteins have been shown to play crucial roles in various events in cell survival and differentiation through organizing actin-based cytoskeletons underlying plasma membranes (Tsukita and Yonemura, 1999; Bretscher et al., 2002). However, the possible involvement of ERM proteins in gastric acid secretion in parietal cells has not been well evaluated. Therefore, we attempted to examine the function of ezrin in gastric acid secretion in parietal cells using gene targeting technology.

Results and discussion

We first generated mice completely lacking the expression of ezrin ($Vil2^{-/-}$ mice). When $Vil2^{+/-}$ mice were interbred, $Vil2^{-/-}$

Correspondence to Sachiko Tsukita: atsukita@mfour.med.kyoto-u.ac.jp

Abbreviations used in this paper: ERM, ezrin/radixin/moesin; HCl, hydrochloric acid.

The Journal of Cell Biology, Vol. 169, No. 1, April 11, 2005 21–28
http://www.jcb.org/cgi/doi/10.1083/jcb.200410083

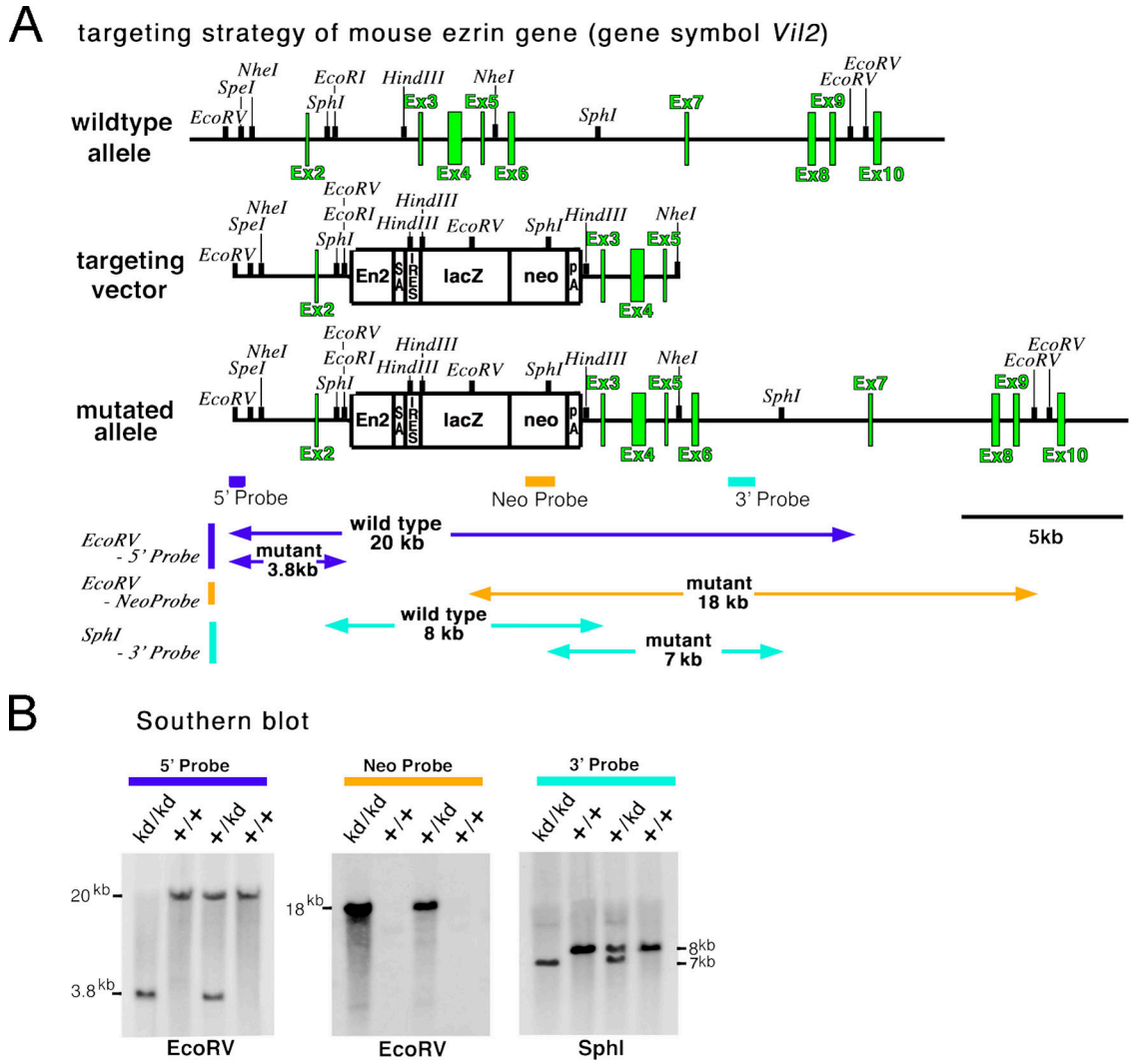

Figure 1. **Generation of ezrin knockdown (*Vil2*$^{kd/kd}$) mice.** (A) Schematic representation of the wild-type allele, targeting vector, and targeted allele of the mouse ezrin gene (*Vil2*). The first ATG codon was located in exon 2. The targeting vector contained the neomycin-resistance cassette (neo) combined with engrailed-2 (En-2)/splicing acceptor (SA)/internal ribosome entry site (IRES)/β-galactosidase (lacZ) on its 5′ side and with a polyadenylation site (PA) on its 3′ side, which was designed to be inserted between exons 2 and 3 in the targeted allele. (B) Southern blot analysis of genomic DNA from wild-type (+/+), heterozygous (+/*kd*), and ezrin knockdown (*kd*/*kd*) mice. The EcoRV fragments were detected by the 5′ probe from wild-type (20 kb) and targeted alleles (3.8 kb), and by the neo probe from targeted alleles (18 kb). The SphI fragments were detected by the 3′ probe from wild-type (8 kb) and targeted alleles (7 kb).

mice were born at the submendelian segregation ratio, but they did not grow, and showed no increase in body weight after birth. All *Vil2*$^{-/-}$ mice died within 1.5 wk after birth before weaning (unpublished data). These findings were consistent with the recent report by Saotome et al. (2004). Considering that gastric acid secretion develops after birth and matures after weaning in mice (Helander, 1970; Ackerman, 1982), we concluded that *Vil2*$^{-/-}$ mice were not suitable for studying the role of ezrin in HCl secretion from parietal cells. We then attempted to produce ezrin knockdown mice (*Vil2*$^{kd/kd}$) in which the expression of ezrin was not completely abolished, but largely suppressed. For that purpose, we targeted embryonic stem cells using a replacement construct that was designed to insert a neomycin-resistance cassette between exons 2 and 3 of the ezrin gene, according to the previous method described previously (Nagai et al., 2000; Fig. 1 A). Correctly targeted cells were selected by Southern blotting with internal and external probes, and by blastocyst injections of two independent embryonic stem cell clones, two lines of mice heterozygous for a mutation in the ezrin locus (*Vil2*$^{+/kd}$) were obtained. When *Vil2*$^{+/kd}$ mice were interbred, wild-type (*Vil2*$^{+/+}$), heterozygous (*Vil2*$^{+/kd}$), and homozygous mutant (*Vil2*$^{kd/kd}$) mice were born at the expected Mendelian segregation ratio, as observed from Southern blots (Fig. 1 B).

Vil2$^{kd/kd}$ mice exhibited severe growth retardation and a high mortality up to the weaning period (~3 wk after birth; Fig. 2 A). However, in contrast to *Vil2*$^{-/-}$ mice, ~7% of *Vil2*$^{kd/kd}$ mice survived beyond the weaning period. These mice gradually increased their body weight, and reached ~75% of the body weight of their wild-type littermates by 7 wk (Fig. 2 B). They survived at least up to 2 yr old, and showed no severe gross abnormalities in histological scan. For example, in *Vil2*$^{kd/kd}$ mice, intestinal villi as well as microvillar structures of intestinal cells appeared to be normal, though they were sometimes

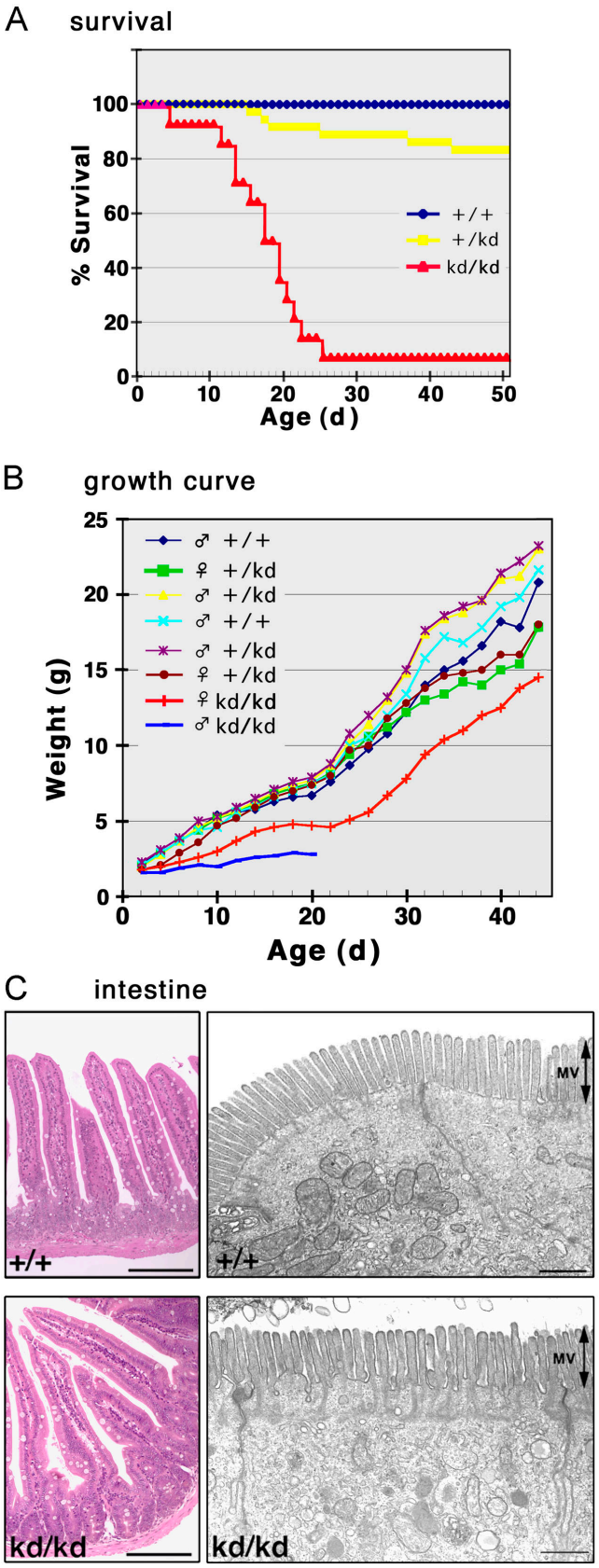

Figure 2. ***Vil2*$^{+/+}$, *Vil2*$^{+/kd}$, and *Vil2*$^{kd/kd}$ mice.** (A) Survival curves of *Vil2*$^{+/+}$, *Vil2*$^{+/kd}$, and *Vil2*$^{kd/kd}$ mice (n = 29 for each group). Approximately 7% of *Vil2*$^{kd/kd}$ mice survived for >25 d to become adults. (B) Growth curves of *Vil2*$^{+/+}$, *Vil2*$^{+/kd}$, and *Vil2*$^{kd/kd}$ mice in one set of littermates from heterozygous mating. (C) Light and electron micrographs of *Vil2*$^{+/+}$ and *Vil2*$^{kd/kd}$ small intestine. At the light microscopic level (left), in *Vil2*$^{kd/kd}$ mice, intestinal villi appear to be normally developed, though they were occasionally deformed. However, ultra-thin section EM identified no significant morphological abnormalities in *Vil2*$^{kd/kd}$ intestinal epithelial cells (right). MV, microvilli. Bars: (left) 50 μm; (right) 1 μm.

slightly deformed (Fig. 2 C). Furthermore, the serum profile in these mice suggested that the intestinal absorption of glucose, trigycerol, cholesterol, or amino acids was not affected (unpublished data).

We then examined the expression of ERM proteins in various organs of adult sex-matched *Vil2*$^{+/+}$ and *Vil2*$^{kd/kd}$ littermate pairs aged ~8 wk. When immunoblotting was performed with anti-ERM pAb, which equally recognized ERM proteins, ezrin was mostly undetectable without compensatory up-regulation of radixin or moesin in most *Vil2*$^{kd/kd}$ organs such as heart, liver, lung, and small intestine (Fig. 3 A). In the *Vil2*$^{kd/kd}$ stomach, a small amount of ezrin was reproducibly detected, possibly because exceptionally large amounts of ezrin are expressed in *Vil2*$^{+/+}$ stomach (Fig. 3 A). Immunoblotting with antibodies specific for ezrin, radixin, or moesin confirmed that in the *Vil2*$^{kd/kd}$ stomach, ezrin was expressed in small amounts (~5%) and that the expression of radixin or moesin was not up-regulated in a compensatory manner (Fig. 3 B). Quantitative RT-PCR analyses revealed that in the *Vil2*$^{kd/kd}$ stomach, ezrin mRNA levels were decreased to <5% of *Vil2*$^{+/+}$ stomach levels (not depicted). The stomach of adult *Vil2*$^{kd/kd}$ mice appeared normal macroscopically. Histological examination of the *Vil2*$^{kd/kd}$ stomach revealed that parietal cells, as well as chief and mucous cells, were normally developed, which were indistinguishable from those in the *Vil2*$^{+/+}$ stomach. However, there was a thickening of the gastric mucosa in *Vil2*$^{kd/kd}$ mice (Fig. 3 C). Ultra-thin section EM also easily identified these differentiated gastric epithelial cell types in the *Vil2*$^{kd/kd}$ stomach (not depicted). Immunofluorescence microscopy revealed that in *Vil2*$^{kd/kd}$ parietal cells, which were positive for H^+,K^+-ATPase, no compensatory up-regulation of radixin or moesin was detected (Fig. 3 D). These findings indicated that the stomach of adult *Vil2*$^{kd/kd}$ mice could provide a useful system to evaluate the possible involvement of ezrin in HCl secretion in parietal cells.

Because the gastric juice of *Vil2*$^{+/+}$ and *Vil2*$^{kd/kd}$ stomachs showed a different pH by strips of pH indicator paper, acidic and neutral, respectively, suggesting that *Vil2*$^{kd/kd}$ mice suffered from achlorhydria (unpublished data), we prepared the isolated stomach samples from adult sex-matched *Vil2*$^{+/+}$ and *Vil2*$^{kd/kd}$ littermate pairs aged 6–20 wk, and measured histamine-triggered acid secretion using the Ussing chamber system (Suzuki and Kaneko, 1987). As shown in Fig. 4 A, when the isolated stomach was stimulated by histamine under physiological conditions, acid secretion was measured as 1.76 ± 0.38 and 0.14 ± 0.21 μmol/h/cm^2 (mean ± SD, n = 4) for the *Vil2*$^{+/+}$ and *Vil2*$^{kd/kd}$ stomach, respectively, confirming achlorhydria in the *Vil2*$^{kd/kd}$ mice.

The question has naturally arisen how the suppression of ezrin expression abolishes HCl secretion in parietal cells. There

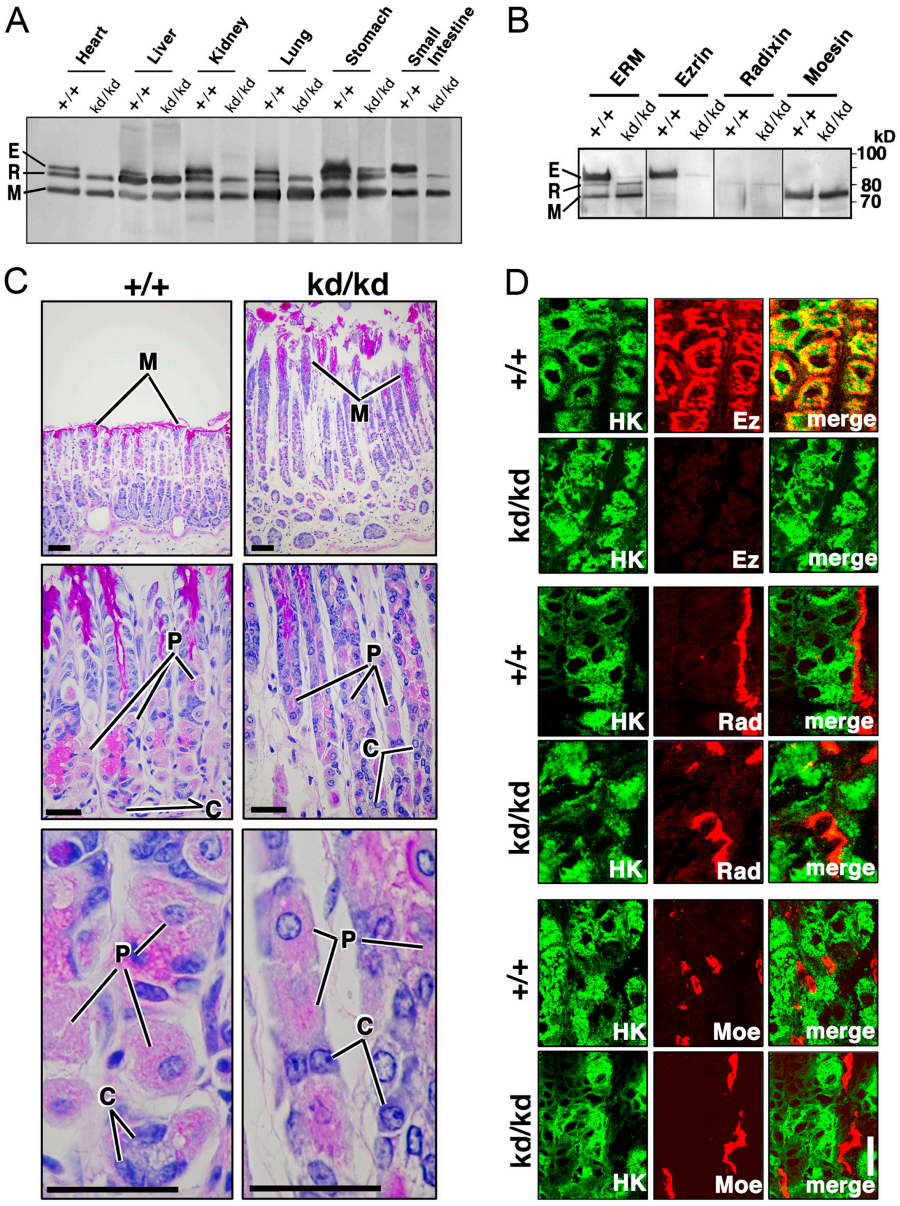

Figure 3. **Stomach of adult *Vil2*$^{+/+}$ and *Vil2*$^{kd/kd}$ mice.** (A) Immunoblotting of various *Vil2*$^{+/+}$ and *Vil2*$^{kd/kd}$ organs with anti-ERM pAb that equally recognizes ezrin (E), radixin (R), and moesin (M). 25 μg of protein of whole lysate was applied onto each lane. Ezrin became undetectable in all organs but the stomach of *Vil2*$^{kd/kd}$ mice. Ezrin was reproducibly detected in small amounts in the *Vil2*$^{kd/kd}$ stomach. No compensatory up-regulation of radixin or moesin was detected. (B) Immunoblotting of *Vil2*$^{+/+}$ and *Vil2*$^{kd/kd}$ stomachs with mAbs specific for ezrin, radixin, or moesin. In the *Vil2*$^{kd/kd}$ stomach, the protein level of ezrin was decreased to <5% of *Vil2*$^{+/+}$ stomach levels. (C) Light microscopic images of hematoxylin-eosin–stained sections of *Vil2*$^{+/+}$ and *Vil2*$^{kd/kd}$ gastric glands. In *Vil2*$^{+/+}$ gastric epithelial cellular sheets, three types of cells, parietal (P), chief (C), and mucous (M) cells, were easily distinguished. In the *Vil2*$^{kd/kd}$ stomach, no abnormality was detected in terms of cellular differentiation, though there was a thickening of the gastric mucosa. Bars, 50 μm. (D) Immunofluorescence micrographs of *Vil2*$^{+/+}$ and *Vil2*$^{kd/kd}$ stomachs. Frozen sections were double stained for H^+,K^+-ATPase (HK)/ezrin (Ez), H^+,K^+-ATPase (HK)/radixin (Rad), and H^+,K^+-ATPase (HK)/moesin (Moe). Note that in *Vil2*$^{kd/kd}$ HK-positive parietal cells, ezrin was almost undetectable, and radixin or moesin was not up-regulated. Bar, 10 μm.

were no differences detected between *Vil2*$^{+/+}$ and *Vil2*$^{kd/kd}$ parietal cells in the expression level and subcellular distribution of gastric H^+,K^+-ATPase (Fig. 4, B and C). In the *Vil2*$^{+/+}$ stomach, ezrin was highly concentrated at the well-developed actin cortical layers of parietal cells (Fig. 4 D). By contrast, in the *Vil2*$^{kd/kd}$ stomach, immunofluorescence signal for ezrin was very weak and it was difficult to determine its subcellular distribution in parietal cells. In these parietal cells, the subcortical actin layer became significantly thinner as compared with that in *Vil2*$^{+/+}$ stomach. As reported previously (Mercier et al., 1989; Agnew et al., 1999; Zhou et al., 2003), when isolated *Vil2*$^{+/+}$ stomach was incubated with histamine, the organization of actin-based cytoskeletons in parietal cells changed markedly (Fig. 4 E). In addition to the cortical layers, the deeper regions of parietal cells were also positive for rhodamine-phalloidine staining. This change was thought to be attributed to the expansion of canalicular apical membranes into the deeper regions through successive tubulovesicle fusion that was associated with the facilitation of actin polymerization beneath these newly formed apical membranes. Interestingly, in parietal cells in the *Vil2*$^{kd/kd}$ stomach, the rhodamine-phalloidine staining pattern, i.e., thin cortical actin layers, did not change significantly with histamine stimulation (Fig. 4 E). This suggested that ezrin knockdown affected the molecular mechanism behind the expansion of canalicular apical membranes in parietal cells.

Finally, we examined the *Vil2*$^{+/+}$ and *Vil2*$^{kd/kd}$ parietal cells by ultra-thin section EM (Fig. 5). We fasted *Vil2*$^{+/+}$ and *Vil2*$^{kd/kd}$ mice in order to suppress the secretion of gastric juice. In the *Vil2*$^{+/+}$ stomach, parietal cells are characterized by a meandering invagination of the apical surface called the secretory canaliculus, which bears numerous microvilli with actin filament cores (Fig. 5 A, red). Tubulovesicles were densely distributed just beneath the apical canalicular membranes (Fig. 5 A, blue). They were similar in dimension and appearance to canalicular microvilli, though they were vacant vesicular structures and not cellular protrusions. Close inspection easily dis-

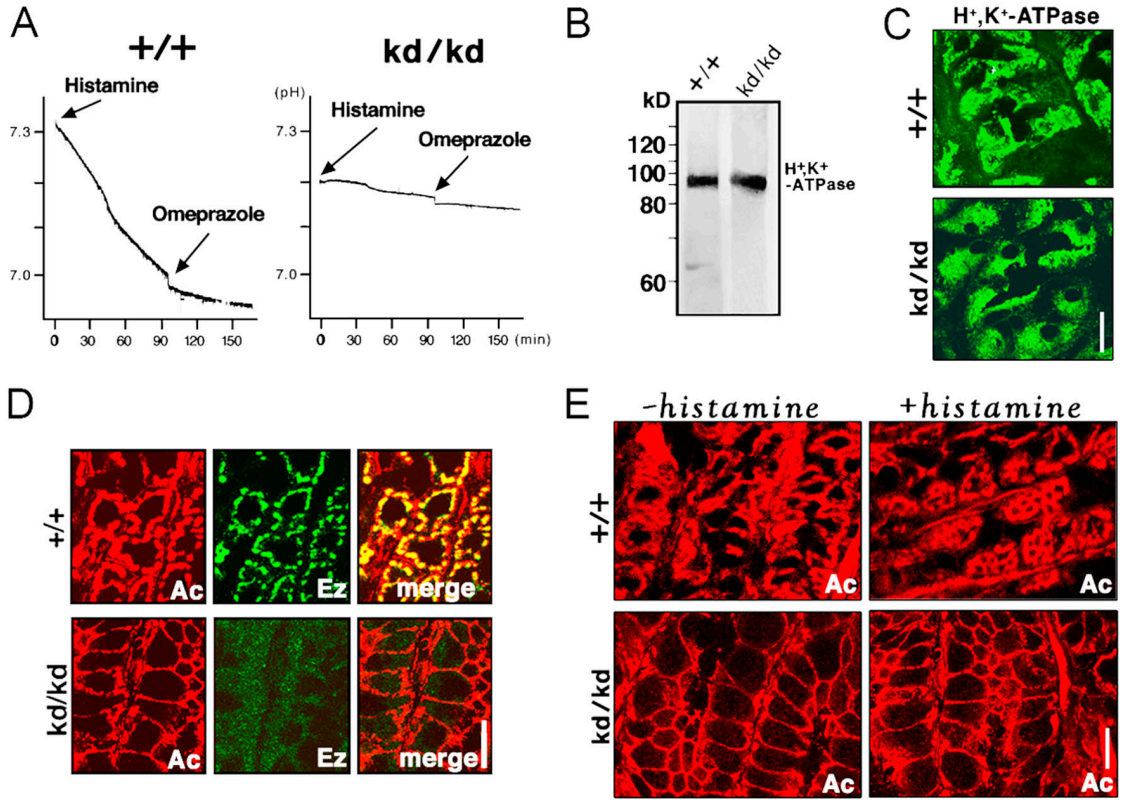

Figure 4. **Acid secretion from *Vil2*$^{+/+}$ and *Vil2*$^{kd/kd}$ stomachs.** (A) Direct measurements of histamine-induced acid secretion. Stomach samples isolated from adult *Vil2*$^{+/+}$ and *Vil2*$^{kd/kd}$ mice were set up in the Ussing chamber: the muscle layer was carefully removed to avoid hypoxia. Acid secretion, which was triggered by addition of histamine from the serosal side, was directly recorded by measuring the pH change in the mucosal side. 100 min after the histamine stimulation, omeprazole was added to the mucosal chamber to specifically inhibit the activity of H^+,K^+-ATPase. Acid secretion was measured as 1.76 ± 0.38 and 0.14 ± 0.21 μmol/h/cm^2 (mean ± SD; $n = 4$) for *Vil2*$^{+/+}$ and *Vil2*$^{kd/kd}$ stomach, respectively. This value obtained from isolated *Vil2*$^{+/+}$ stomach was comparable to the previously reported value from in vivo wild-type stomach (Hasebe et al., 2001; Piqueras et al., 2003). (B) Immunoblotting of adult *Vil2*$^{+/+}$ and *Vil2*$^{kd/kd}$ stomachs with anti-H^+,K^+-ATPase mAb. No change was detected in protein levels of H^+,K^+-ATPase. (C) Subcellular distribution of H^+,K^+-ATPase in *Vil2*$^{+/+}$ and *Vil2*$^{kd/kd}$ stomachs. Frozen sections were immunofluorescently stained with anti-H^+,K^+-ATPase mAb. In *Vil2*$^{+/+}$ parietal cells, H^+,K^+-ATPase was diffusely distributed in the cytoplasm, which did not appear to be affected by ezrin knockdown. Bar, 10 μm. (D) Immunofluorescence micrographs for actin and ezrin in *Vil2*$^{+/+}$ and *Vil2*$^{kd/kd}$ stomach, ezrin signals overlapped with actin signals from well-developed subcortical actin layers of parietal cells. Note that in the *Vil2*$^{kd/kd}$ stomach, ezrin became mostly undetectable and the subcortical actin layers were significantly thinner as compared with those in *Vil2*$^{+/+}$ stomach. Bar, 10 μm. (E) Actin organization of *Vil2*$^{+/+}$ and *Vil2*$^{kd/kd}$ parietal cells before and after histamine stimulation. Isolated *Vil2*$^{+/+}$ and *Vil2*$^{kd/kd}$ stomachs were frozen without histamine stimulation (−histamine) or at a 15-min incubation with histamine (+histamine), and frozen sections were stained with rhodamine-phalloidin (Ac). In *Vil2*$^{+/+}$ parietal cells, histamine stimulation induced significant expansion of actin-positive regions from the subcortical to the deeper regions. In contrast, the thin subcortical actin layer of *Vil2*$^{kd/kd}$ parietal cells did not respond to histamine stimulation. Bar, 10 μm.

tinguished these two membranous structures (Fig. 5 A). *Vil2*$^{+/+}$ parietal cells bore a fairly developed secretory canaliculus in addition to cytoplasmic tubulovesicles. In contrast, *Vil2*$^{kd/kd}$ parietal cells mostly lacked invaginated apical canaliculi, with the cytoplasm filled with numerous tubulovesicles (Fig. 5 B, −histamine). The stomach, which was dissected out from fasted *Vil2*$^{+/+}$ and *Vil2*$^{kd/kd}$ mice, was stimulated with histamine (Fig. 5 B, +histamine). In histamine-stimulated *Vil2*$^{+/+}$ parietal cells, the apical secretory canaliculus markedly expanded, and tubulovesicles were decreased in number, though the size and morphological aspects of the remaining tubulovesicles did not change. However, in *Vil2*$^{kd/kd}$ parietal cells, histamine stimulation did not induce the formation/expansion of apical secretory canaliculi, leaving the cytoplasm densely packed with tubulovesicles. This difference in the behavior of the apical canalicular membrane and tubulovesicles between *Vil2*$^{+/+}$ and *Vil2*$^{kd/kd}$ parietal cells was confirmed semi-quantitatively (Fig. 5 C). Therefore, we concluded that ezrin is not required for formation of tubulovesicles per se, but plays a crucial role in formation/expansion of apical secretory canaliculi in parietal cells. This formation/expansion process may include many steps such as signaling, recruitment/docking/fusion of tubulovesicles to apical membranes, etc. It is still premature to further discuss how ezrin is involved in the secretion of gastric acid at the molecular level, but we believe that *Vil2*$^{kd/kd}$ mice, as well as radixin-deficient mice (Kikuchi et al., 2002), will offer novel systems to understand how ERM proteins are involved in the formation of epithelial apical membranes in general.

Materials and methods

Antibodies and reagents

Rabbit anti-ERM pAb (TK89) recognized all ERM proteins almost equally (Kondo et al., 1997). Rat anti-ezrin, anti-radixin, and anti-moesin mAbs reacted specifically with the respective ERM proteins (Kondo et al., 1997). Anti–α-subunit of H^+,K^+-ATPase mAb (Calbiochem), anti–β-subunit of H^+, K^+-ATPase mAb (Affinity BioReagents), histamine, and omeprazole (Sigma-Aldrich) were purchased.

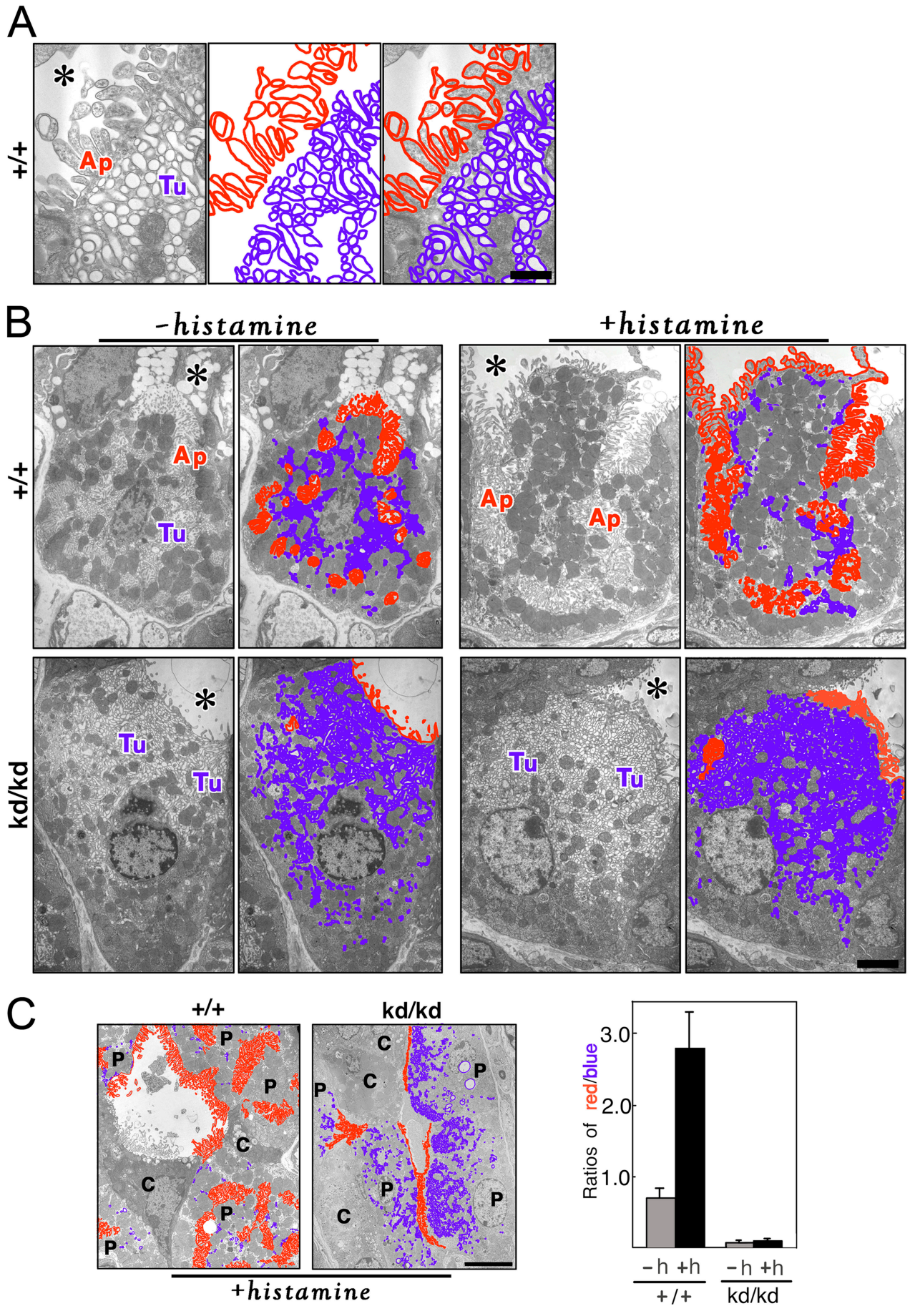
A
+/+
Ap
Tu
B
-histamine
+histamine
+/+
kd/kd
Ap
Tu
C
+/+
kd/kd
P
C
+histamine
Ratios of red/blue
3.0
2.0
1.0
-h +h
-h +h
+/+
kd/kd

Generation of ezrin knockdown (Vil2$^{kd/kd}$) mice

The ezrin genomic clone (13.7 kb) including exons 2–6 was isolated from a λ-phage 129/Sv mouse genomic library. The targeting vector (Fig. 1 A) was constructed by standard recombinant DNA techniques and the ezrin knockdown mice were obtained as described previously (Doi et al., 1999; Nagai et al., 2000; Kikuchi et al., 2002).

Immunoblotting

Various tissues were taken from *Vil2*$^{kd/kd}$ and *Vil2*$^{+/+}$ mice and homogenized in SDS sample buffer (50 mM Tris-HCl, pH 6.8, 2% SDS, 20% glycerol, 2% 2-mercaptoethanol, 0.01% bromophenol blue). Total lysates (25 μg) were separated by SDS-PAGE (10% SDS-PAGE). Proteins were then electrophoretically transferred from gels to nitrocellulose membranes and then processed for immunoblotting. Representative data were obtained from the independent immunoblots for five separate combinations of *Vil2*$^{kd/kd}$ and *Vil2*$^{+/+}$ mice.

Immunofluorescence microscopy

Organs from *Vil2*$^{kd/kd}$ and *Vil2*$^{+/+}$ mice were cut into small pieces and frozen in liquid nitrogen for immunofluorescence microscopy. Frozen sections of *Vil2*$^{kd/kd}$ and *Vil2*$^{+/+}$ stomachs were cut on a cryostat, mounted on glass slides, and air dried. They were fixed with 100% methanol at −20°C for 10 min or 2% formaldehyde in PBS at RT for 15 min, and processed for immunofluorescence microscopy. Fluorescence images were obtained with a confocal microscope (model LSM 510 META; Carl Zeiss MicroImaging, Inc.), equipped with an Axioplan2 (Plan Apochromat 63×/1.40 NA oil immersion objective; Carl Zeiss MicroImaging, Inc.).

EM

Vil2$^{kd/kd}$ and *Vil2*$^{+/+}$ stomach samples were fixed in 2.5% glutaraldehyde and 2% formaldehyde in 0.1 M cacodylate buffer, pH 7.2, and processed for ultra-thin section EM as described previously (Kikuchi et al., 2002).

Histamine stimulation and measurement of acid secretion in the Ussing chamber

The gastric region of the stomach was cut off and the muscle layer was largely removed with fine scissors. The resultant tissue preparations were mounted vertically between chambers that provided an exposed area of 0.2 cm^2. The volume of the bathing solution in each side was 15 ml. The temperature of the bathing solution was kept at 37°C. The serosal bathing solution (119 mM NaCl, 21 mM $NaHCO_3$, 2.4 mM K_2HPO_4, 0.6 mM KH_2PO_4, 1.2 mM $CaCl_2$, 1.2 mM $MgCl_2$, and 10 mM glucose) was gassed with 95% O_2/5% CO_2, pH 7.3–7.4. The mucosal bathing solution (140 mM NaCl, 5.4 mM KCl, 1.2 mM $CaCl_2$, 1.2 mM $MgCl_2$, 0.5 mM Hepes, pH 7.4, and 10 mM glucose) was gassed with 100% O_2. The H^+ secretion rate was determined from the pH change in the mucosal bathing solution and the titration curve of the solution. The pH was monitored using a combined pH electrode (GS-5015C; DKK-TOA). Histamine (1 mM) was added to the serosal side and omeprazole (200 μM), a gastric H^+,K^+-ATPase inhibitor, was added to the mucosal side.

This work was supported in part by a grant-in-aid for Scientific Research (B) (to Sa. Tsukita) and a grant-in-aid for Cancer Research (to Sh. Tsukita) from the Ministry of Education, Science and Culture of Japan.

Submitted: 15 October 2004
Accepted: 9 February 2005

References

Ackerman, S.H. 1982. Ontogeny of gastric acid secretion in the rat: evidence for multiple response systems. *Science.* 217:75–77.

Agnew, B.J., J.G. Duman, C.L. Watson, D.E. Coling, and J.G. Forte. 1999. Cytological transformations associated with parietal cell stimulation: critical steps in the activation cascade. *J. Cell Sci.* 112:2639–2646.

Bretscher, A. 1983. Purification of an 80,000-dalton protein that is a component of the isolated microvillus cytoskeleton, and its localization in nonmuscle cells. *J. Cell Biol.* 97:425–432.

Bretscher, A., K. Edwards, and R.G. Fehon. 2002. ERM proteins and merlin: integrators at the cell cortex. *Nat. Rev. Mol. Cell Biol.* 3:586–599.

Doi, Y., M. Itoh, S. Yonemura, S. Ishihara, H. Takano, T. Noda, Sh. Tsukita, and Sa. Tsukita. 1999. Normal development of mice and unimpaired cell adhesion/cell motility/actin-based cytoskeleton without compensatory up-regulation of ezrin or radixin in moesin gene knockout. *J. Biol. Chem.* 274:2315–2321.

Duman, J.G., N.J. Pathak, M.S. Ladinsky, K.L. McDonald, and J.G. Forte. 2002. Three-dimensional rsconstruction of cytoplasmic membrane networks in parietal cells. *J. Cell Sci.* 115:1251–1258.

Forte, J.G., and X. Yao. 1996. The membrane-recruitment-and-recycling hypothesis of gastric HCl secretion. *Trends Cell Biol.* 6:45–48.

Forte, T.M., T.E. Machen, and J.G. Forte. 1977. Ultrastructural changes in oxyntic cells associated with secretory function: a membrane-recycling hypothesis. *Gastroenterology.* 73:941–955.

Hanzel, D., H. Reggio, A. Bretscher, J.G. Forte, and P. Mangeat. 1991. The secretion-stimulated 80K phosphoprotein of parietal cells is ezrin, and has properties of a membrane cytoskeletal linker in the induced apical microvilli. *EMBO J.* 10:2363–2373.

Hasebe, K., S. Horie, M. Komasaka, S. Yano, and K. Watanabe. 2001. Stimulatory effects of nitric oxide donors on gastric acid secretion in isolated mouse stomach. *Eur. J. Pharmacol.* 420:159–164.

Helander, H.F. 1970. Gastric acidity in young and adult mice. *Scand. J. Gastroenterol.* 5:221–224.

Kikuchi, S., M. Hata, K. Fukumoto, Y. Yamane, T. Matsui, A. Tamura, S. Yonemura, H. Yamagishi, D. Keppler, Sh. Tsukita, and Sa. Tsukita. 2002. Radixin deficiency causes conjugated hyperbilirubinemia with loss of Mrp2 from bile canalicular membranes. *Nat. Genet.* 31:320–325.

Kondo, T., K. Takeuchi, Y. Doi, S. Yonemura, S. Nagata, Sh. Tsukita, and Sa. Tsukita. 1997. ERM (ezrin/radixin/moesin)-based molecular mechanism of microvillar breakdown at an early stage of apoptosis. *J. Cell Biol.* 139: 749–758.

Lindstrom, E., D. Chen, P. Norlen, K. Andersson, and R. Hakanson. 2001. Control of gastric acid secretion: the gastrin-ECL cell-parietal cell axis. *Comp. Biochem. Physiol. A Mol. Integr. Physiol.* 128:505–514.

Mercier, F., H. Reggio, G. Devilliers, D. Bataille, and P. Mangeat. 1989. Membrane-cytoskeleton dynamics in rat parietal cells: mobilization of actin and spectrin upon stimulation of gastric acid secretion. *J. Cell Biol.* 108: 441–453.

Nagai, T., J. Aruga, O. Minowa, T. Sugimoto, Y. Ohno, T. Noda, and K. Mikoshiba. 2000. Zic2 regulates the kinetics of neurulation. *Proc. Natl. Acad. Sci. USA.* 97:1618–1623.

Piqueras, L., Y. Tache, and V. Martinez. 2003. Somatostatin receptor type 2 mediates bombesin-induced inhibition of gastric acid secretion in mice. *J. Physiol.* 549:889–901.

Saotome, I., M. Curto, and A.I. McClatchey. 2004. Ezrin is essential for epithelial organization and villus morphogenesis in the developing intestine.

Figure 5. **Ultra-thin section EM of parietal cells in adult *Vil2*$^{+/+}$ and *Vil2*$^{kd/kd}$ mice.** (A) Microvilli versus tubulovesicles in *Vil2*$^{+/+}$ parietal cells. In *Vil2*$^{+/+}$ parietal cells, the apical membranes (Ap) are invaginated in a complicated manner, from which numerous microvilli are projected into the luminal space (asterisk). These microvilli bear actin filament cores. Numerous tubulovesicles (Tu) occur just beneath the apical plasma membranes and they appear similar to microvilli in dimension and appearance, but they are vacant vesicles, not cellular protrusions. Based on these morphological characteristics, we marked apical microvilli and tubulovesicles in red and blue, respectively. Bar, 0.5 μm. (B) Microvilli versus tubulovesicles in parietal cells of fasted *Vil2*$^{+/+}$ and *Vil2*$^{kd/kd}$ mice before or after histamine stimulation. Isolated *Vil2*$^{+/+}$ and *Vil2*$^{kd/kd}$ stomachs were fixed without histamine stimulation (−histamine) or at a 15-min incubation with histamine (+histamine), and samples were observed by ultra-thin section EM. Apical microvilli (Ap) and tubulovesicles (Tu) were marked in red and blue, respectively. Before histamine stimulation (−histamine), *Vil2*$^{+/+}$ parietal cells were characterized by deeply invaginated apical membranes, i.e., secretory canaliculi (red), and tubulovesicles (blue) in the cytoplasm, whereas *Vil2*$^{kd/kd}$ parietal cells mostly lacked secretory canaliculi (red) and were filled with numerous tubulovesicles (blue). In *Vil2*$^{+/+}$ parietal cells, histamine stimulation (+histamine) facilitated the fusion of tubulovesicles to apical canalicular membranes, resulting in the remarkable decrease in the number of tubulovesicles in the cytoplasm. In contrast, in *Vil2*$^{kd/kd}$ parietal cells, apical canalicular membranes (red) did not develop with histamine stimulation (+histamine), and the cytoplasm was still filled with numerous tubulovesicles (Tu, blue). Bar, 2 μm. (C) Semi-quantitative analyses. In *Vil2*$^{+/+}$ and *Vil2*$^{kd/kd}$ parietal cells, apical membranes and tubulovesicles were marked in red and blue, respectively, in low magnification electron micrographs before (not depicted) and after (left) histamine stimulation. The lengths of red and blue lines were measured in 15 parietal cells from three *Vil2*$^{+/+}$ or *Vil2*$^{kd/kd}$ mice (five cells/each mouse) before or after histamine stimulation, and the red/blue ratios were calculated. Error bars indicate SD. Bar, 10 μm.

Dev. Cell. 6:855–864.

Sato, N., N. Funayama, A. Nagafuchi, S. Yonemura, Sa. Tsukita, and Sh. Tsukita. 1992. A gene family consisting of ezrin, radixin and moesin. Its specific localization at actin filament/plasma membrane association sites. *J. Cell Sci.* 103:131–143.

Suzuki, Y., and K. Kaneko. 1987. Acid secretion in isolated guinea pig colon. *Am. J. Physiol.* 253:G155–G164.

Tsukita, Sa., and S. Yonemura. 1999. Cortical actin organization: lessons from ERM (ezrin/radixin/moesin) proteins. *J. Biol. Chem.* 274:34507–34510.

Urushidani, T., and J.G. Forte. 1997. Signal transduction and activation of acid secretion in the parietal cell. *J. Membr. Biol.* 159:99–111.

Yao, X., and J.G. Forte. 2003. Cell biology of acid secretion by the parietal cell. *Annu. Rev. Physiol.* 65:103–131.

Zhou, R., X. Cao, C. Watson, Y. Miao, Z. Guo, J.G. Forte, and X. Yao. 2003. Characterization of protein kinase A-mediated phosphorylation of ezrin in gastric parietal cell activation. *J. Biol. Chem.* 278:35651–35659.